Seismic Three Dimensional Stability of Reinforced Slopes

Faradjollah Askari

Assistant Professor, Geotechnical Engineering Research Center, International Institute of Earthquake Engineering and Seismology (IIEES), email: askari@iiees.ac.ir

Received: 07/07/2013
Accepted: 17/11/2013

ABSTRACT

Upper bound limit analysis method is applied to determine the required reinforcement for three-dimensional stability of the slopes under seismic conditions. Horizontal blocks are used for determining the internal stability in three-dimensional conditions. Seismic stability is studied by adopting a pseudo-static approach, considering only the horizontal acceleration. Reinforced soil has been considered to be a cohesionless material in the analysis. The failure mechanism is considered to be transitional and consists of several horizontal hexagonal blocks and a pentagonal one at the base. Velocity discontinuities between blocks are considered to be horizontal and each block consists of one reinforcement layer. Results are presented in graphical and tabular form to illustrate the effects of variation of different parameters such as seismic acceleration, three-dimensional geometry of the slope and soil friction angle on required reinforcement length and strength. By increasing of seismic acceleration, the stability of the reinforced soil slope decreases significantly, and thus greater strength and length of the reinforcement are required to maintain stability of the slope. On the other hand, three-dimensional modeling of reinforced slope results lower values of the required reinforcement. Comparisons of the present results with available pseudo-static results are shown, and discussed.

Keywords:
Reinforced slopes; Three dimensional analysis; Seismic slope stability; Limit analysis

1. Introduction

Reinforced soils have been in use for more than three decades, and reinforcement of soil structures such as slopes and walls as well as stability analysis of such structures has been the subject of a lot of experimental and analytical studies.

The analytical methods usually considered in slope stability studies are limit equilibrium, limit analysis and characteristics methods. Although a lot of analytical models have been considered for design of reinforced slopes, the most common analytical method up to now has been the 'limit equilibrium' method. On the other hand, available methods for the seismic design of reinforced soil walls and slopes are usually based on the pseudo-static method analysis.

Ling et al. [1] have proposed some seismic design procedures for geosynthetic-reinforced soil structures based on pseudo-static limit equilibrium. In their study, stability analyses have been conducted to determine the required strength and length of reinforcement. Nouri et al. [2] have proposed a failure mechanism consisting of horizontal sliding blocks based on limit equilibrium method to determine the required strength and length of reinforcement.

Michalowski [3-4] applied the upper bound limit analysis theorem and calculated the strength and length of the necessary reinforcement to prevent the collapse of slopes under the assumption that the reinforcement strength is uniformly distributed through the slope height or linearly increasing with

depth. He determined the required strength of reinforcement using rotational log-spiral mechanism and the length of reinforcement using both rotational and direct sliding mechanisms.

Some other important studies in this field, which may be referred to are the ones performed by Shahgholi et al. [5], Kramer and Paulsen [6], El-Emam and Bathurst [7], Huang and Wang [8], Shukla et al. [9], Li et al. [10], Jiang et al. [11], Ghanbari and Taheri [12] and Vieira et al. [13].

As mentioned above, stability of reinforced slopes has generally been analyzed two-dimensionally, assuming plane strain conditions. However, the failure lengths of the slopes have finite dimensions in many practical problems and three-dimensional approach may be more appropriate to analyze such problems.

The common approach to 3D slope stability evaluation has also been the limit-equilibrium method and a few procedures are available based on limit analysis method. Currently, limit analysis has been employed to deal with 3D slope stability problems by Michalowski [14], Chen et al. [15], Farzaneh and Askari [16], and Li et al. [17]. The method was developed numerically by Lyamin and Sloan [18] and Krabbenhoft et al. [19].

Recently, the 3D analysis of slopes developed by Farzaneh and Askari [16] was extended to study the 3D stability of the reinforced slopes by limit analysis method by Zohdi [20]. However, by reviewing the researches conducted, it can be concluded that three-dimensional analysis of reinforced soil slopes need further investigations.

In this study, the kinematic theorem of limit analysis is applied to calculate the required reinforcement to ensure the three-dimensional stability of the reinforced slopes with geosynthetic layers. The method may be considered as an extension of Farzaneh and Askari [16], and results are obtained using some of the methods used by Zohdi [20]. After a brief review of the limit analysis theory, a translational failure mechanism is introduced, divided into a number of rigid horizontal slices containing reinforcements. The reinforcements have no direct influence on the inter-slice forces. The possible failure mechanisms with different shapes are considered, and analytical expressions are derived to obtain the required reinforcement to prevent slope from collapse. Comparisons of results with some of those existing in literature for 2D stability analyses are shown, and the most significant differences are indicated. Results for seismic 3D stability analyses are also presented to illustrate the effect of soil characteristics, horizontal pseudo coefficient of acceleration and the geometrical parameters of the slopes on the stability of reinforced earth structures.

2. Limit Analysis Theorems

The theorems of limit analysis (upper and lower bound) constitute powerful tools to find the limit loads in stability problems. The following assumptions are made in this method:

- The material is perfectly plastic
- The limit state can be described by a convex yield function $f(\sigma_{ij}) = 0$ in stress space σ_{ij}
- The material obeys the associated flow rule (normality condition):

$$\dot{\varepsilon}_{ij}^{p} = \dot{\lambda}\frac{\partial f(\sigma_{ij})}{\partial \sigma_{ij}} \tag{1}$$

where $\dot{\varepsilon}_{ij}^{p}$ is the plastic strain rate tensor of the soil, σ_{ij} is the stress tensor, and $\dot{\lambda}$ is a non-negative multiplier that is positive when plastic deformations occur.

The lower bound theorem states that if a stress field, covering the whole body is in equilibrium with the surface tractions and body forces, and does not violate the yield criterion at any point, collapse does not occur. Such stress distributions are called admissible stress fields and supply loads, which are smaller than the true limit load.

For expressing the upper bound theorem, assume a set of external loads acts on a failure mechanism. According to the upper bound theorem, for a kinematically admissible velocity field, an upper bound of the collapse load can be obtained by equating the power dissipated internally in an increment of displacement to the power expended by the external loads. Such kinematically admissible velocity fields have to comply with the kinematical boundary conditions and compatibility conditions following flow rule, Eq. (1).

Modeling the soil as a perfectly plastic material obeying the associated flow rule, theorems of limit analysis may be extended to solve the stability problems in soil mechanics.

The consequence of applying the normality condition to a frictional soil with an internal friction angle of ϕ will be a necessary occurrence of a volume expansion with an angle of dilatation $\psi = \phi$ during the plastic flow. Frictional soils are found experimentally to dilate at increments considerably less than those predicted by the normality condition, that is, $\psi < \phi$. Hence, real soils do not obey the associative flow rule. However, in a large number of stability problems in soil mechanics such as slope stability, lateral earth pressure and bearing capacity problems, deformation conditions are not so restrictive and the soil deformation properties does not affect the collapse load largely. Therefore, the adoption of the limit analysis approach and the associated flow rule in soils appears to be reasonably justified.

The approach used in this paper is based on the upper-bound theorem and can be used to analyze the stability of reinforced slopes.

3. Model of Analysis

The 3D mechanism, used in this study is shown in Figure (1). This mechanism includes rigid transitional horizontal blocks separated by planar velocity discontinuity surfaces. The width of the failure mechanism is limited to lateral surfaces that have orientation ξ with respect to the vertical symmetry plane. The lateral planes are defined so that the compatibility conditions between velocity discontinuity surfaces are satisfied [16]. The applied mechanism consists of several hexagonal blocks and a pentagonal block at the bottom of mechanism. The planar velocity discontinuity surfaces can be defined by points $A_{1(i)}$ to $A_{4(i)}$.

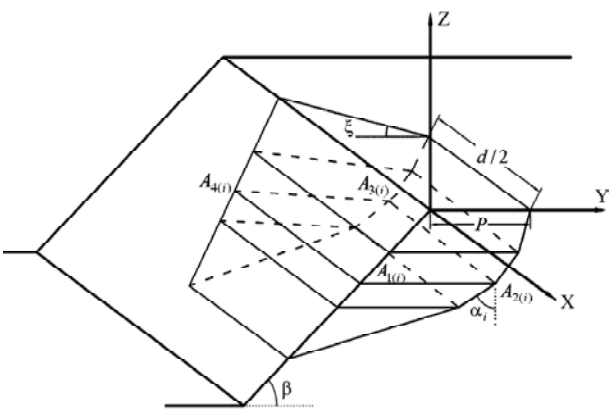

Figure 1. 3D transitional multi-block mechanism used in this study.

In Figure (2), the schematic vertical section in y-z plane is shown. In this Figure, *L* is the total length of the reinforcement, and *le* and *lc* are the length outside and inside the failure zone, respectively. In this Figure, different possible states of the failure mechanism relative to the soil reinforcements are shown. This section is usually used in 2D Analyses.

The horizontal sections of the slope in xoy plane in different levels are shown in Figure (3) [20]. In Figure (3a), the failure surface does not intersect the reinforcement surface (as *le* = 0 in Figure (2)). In case (b), only lateral parts of the reinforcement take part in stabilizing the slope. Finally, in cases (c) and (d), the reinforcement surface is bigger than the failure surface in shown section; however, the part of the reinforcement that is out of the failure surface is not enough and it may pull out before rupture.

For calculation of required reinforcement strength in this paper, it is assumed that the length of reinforcement layers is long enough that the rupture

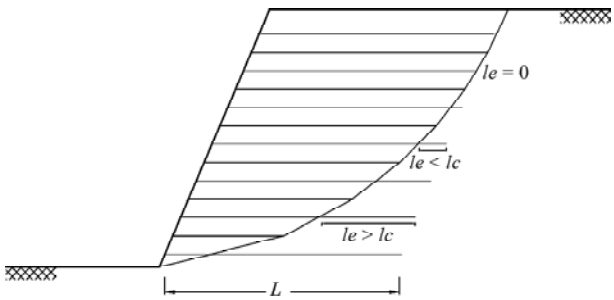

Figure 2. Schematic vertical section of the reinforced slope in Figure (1).

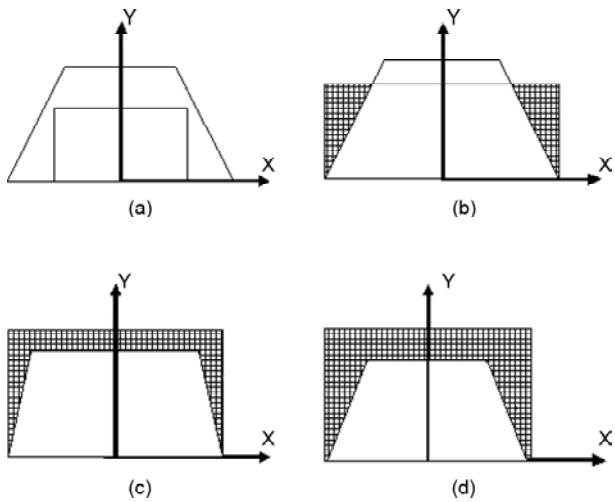

Figure 3. Different possible situations of the reinforcement and the failure surface in a horizontal section of a 3D analysis [20].

collapse occurs at the whole reinforcement layers in unstable conditions (case (d) in Figure (3)).

The distribution of tensile stress along the reinforcement rupture, which is the intersections of reinforcement with two lateral and one bottom slip surfaces, is illustrated in Figure (4).

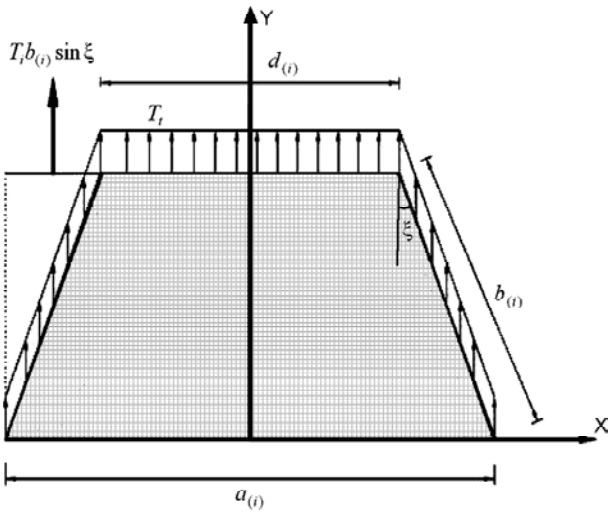

Figure 4. Tensile strength distribution over reinforcement velocity discontinuity boundaries.

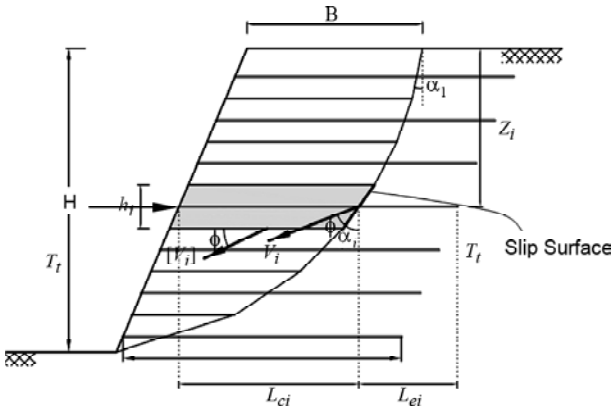

Figure 5. Transitional multi-block mechanism.

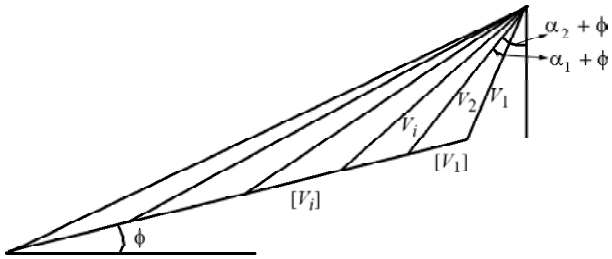

Figure 6. Velocity hodograph for transitional multi-block mechanism.

Based on this assumption, the sum of energy rate dissipated by reinforcement's tensile forces can be shown as follows:

With respect to Figure (4) the tensile force of (i)th reinforcement layer in Y direction, which resists against slope instability, can be obtained using:

$$T_{(i)} = d_{(i)} T_{(t)} + 2b_{(i)} T_{(t)} \sin\xi = T_{(t)} d_{(i)} + T_{(t)} (a_{(i)} - d_{(i)}) = T_{(t)} a_{(i)} \quad (2)$$

where $T_{(i)}$ is the tensile strength of the single reinforcement layer per unit width. $a_{(i)}, b_{(i)}$ and $d_{(i)}$ are geometric parameters of $(i)^{th}$ reinforcement layer, and ξ is a geometric parameter of the failure mechanism.

The transitional multi-block mechanism has been applied to obtain the requirements of reinforcement, Figure (5). In this failure mode, the (i)th rigid block including one reinforcement layer, slides over the failure surface and lower block with velocities V_i and $[V_i]$, respectively, Figure (6).

The amount of absolute velocity of (i)th horizontal block V_i and relative velocity of $(i+1)^{th}$ block with respect to (i)th one ($[V_i]$) can be obtained as follow:

$$V_{i+1} = \frac{\cos(\alpha_i + \phi)}{\cos(\alpha_{i+1} + \phi)} V_i \quad (3)$$

$$[V_i] = \frac{\cos(\alpha_1 + 2\phi)\sin(\alpha_{i+1} - \alpha_i)}{\cos(\alpha_{i+1} + 2\phi)\cos(\alpha_i + 2\phi)} V_i \quad (4)$$

Ignoring the reinforcement mass, the work rate of block's weights and the horizontal seismic forces can be obtained respectively as:

$$\dot{W}_\gamma = \sum_{i=1}^{n} w_i V_i \cos(\alpha_i + \phi) \quad (5)$$

$$\dot{W}_e = \sum_{i=1}^{n} k_h w_i V_i \sin(\alpha_i + \phi) \quad (6)$$

where w_i is the weight of the (i)th block, V_i is the absolute velocity of the (i)th horizontal block, k_h is the horizontal seismic coefficient, α_i is identified at Figure (5), and ϕ is the internal friction of the soil.

For calculation of required reinforcement strength, it is assumed that the length of reinforcement layers is long enough that in the unstable conditions, the rupture collapse occurs at the whole reinforcement layers. Based on this assumption, the sum of energy rate dissipated by reinforcement's tensile forces can be shown as follow:

$$D = \sum_{i=1}^{n} T_{(i)} V_i \sin(\alpha_i + \phi) = \sum_{i=1}^{n} T_t a_{(i)} V_i \sin(\alpha_i + \phi) \quad (7)$$

where n is the number of blocks. Since the amount of reinforcement is assumed to be distributed uniformly through the slope height, the average strength of the reinforcement per unit height can be presented as:

$$k_t = \frac{nT_t}{H} \quad (8)$$

Following expression can be obtained by substitution of the expression $T_{(i)}$ in Eq. (7) with the expression $\frac{H}{n} k_t$ as a result of Eq. (8):

$$\dot{D} = \frac{H}{n} k_t \sum_{i=1}^{n} a_{(i)} V_i \sin(\alpha_i + \phi) \quad (9)$$

Based on kinematic method of limit analysis theorem, the rate of work done by body forces is less than or equal to the rate of energy dissipation in any kinematically admissible failure mechanism [4]. One may solve this inequality and obtain a lower bound value for average strength of the reinforcement (k_t) as follows:

$$k_t = \frac{n}{H} \times \frac{\sum_{i=1}^{n} w_i V_i \cos(\alpha_i + \phi) + \sum_{i=1}^{n} k_h w_i V_i \sin(\alpha_i + \phi)}{\sum_{i=1}^{n} a_{(i)} V_i \sin(\alpha_i + \phi)} \quad (10)$$

This equation provides a lower-bound solution for the reinforcement force necessary to prevent the failure of the slope in a three-dimensional condition. In order to find the best estimation of k_t, an optimization procedure needs to be used to maximize k_t with respect to α_i ($i = 1$ to n), P, d and ξ, Figure (1).

In this study, the average required reinforcement strength for stability in two and three-dimensional conditions are calculated based on above assumptions. For determination of required reinforcement length, in addition to mentioned assumptions, more other assumptions must be made. However, in this study, we have focused on the conditions influence on the amount of required reinforcement strength to prevent slope failure.

It should be mentioned that the current algorithm is more efficient for steep reinforced slopes (with an angle larger than about 70°), which are common in actual civil engineering practice.

4. Verification of the Method

To verify the current method, no analytical results were available for comparison in 3D conditions. Thus, the applied method was verified by comparing the results of the current formulation in 2D conditions with those from existing solutions in the literature. The current method can be compatible to slope analysis in 2D condition in the case of very large width to height ratios (for example $d/H > 1000$). Different slopes were analyzed using the current method and the results were compared with those of the procedures presented in the literature such as Ling et al. [1], Michalowski [4], and Nouri et al. [2].

Comparison of the results obtained in this study to those presented by Ling et al. [1] and Michalowski [4] is given in Figure (7) for a vertical slope $\beta = 90°$. In the calculations performed for verification, the height of slope and the soil density are assumed to be 10 m and 20 kN/m^3, respectively. Figure (7) compares the values of k_t obtained in this study with those proposed by Ling et al. [1] and Michalowski [4]. As seen in Figure (7), the used formulations in this study provide values for k_t that are in close agreement with those read from the graphs by Ling et al. [1] and Michalowski [4]. The obtained results are closely between those by Ling et al. [1] and Michalowski [4]. The difference between the results of the current and Michalowski's method increases as the value of decreases ϕ. Results of Ling et al. [1] are very close together for ϕ values less than 25° and more than 35°. Generally, increasing the angle of internal friction of soil from 20 to 40 degrees, the minimum reinforcement required for the stability of the slope will be reduced to about one-third.

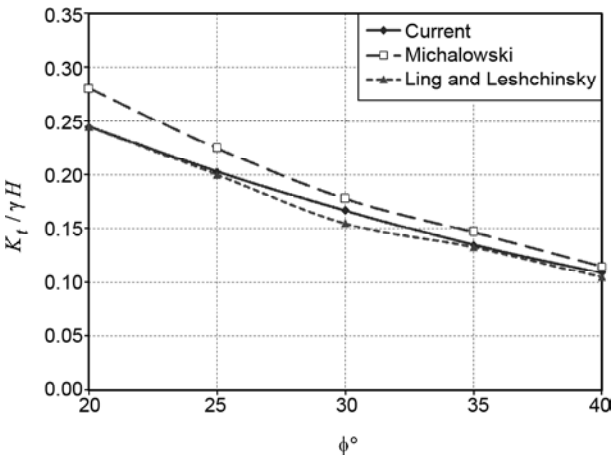

Figure 7. Comparison of required reinforcement strength $\beta = 90°$.

Another comparison of the results of this study to those presented by Nouri et al. [2] is given in Figure (8) for a vertical slope. The results are compared for the seismic coefficient $k_h = 0.2$. As seen in Figure (8), k_t values from the both studies are in a very close agreement.

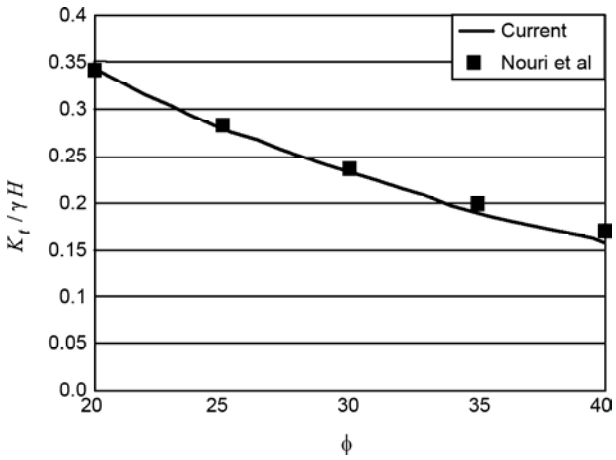

Figure 8. Comparison of required reinforcement strength results of this study to those presented by Nouri et al. [2] for a vertical slope (β = 90°).

5. Results and Discussion

In this section, a parametric study is conducted to illustrate the effect of seismic two and three-dimensional conditions on the required reinforcement strength and lengths and also on stability of the reinforced slopes. The soil is assumed to be cohesionless.

6. Required Reinforcement Length in 2D Cases

Equations (8) and (10) can be used to arrive at the lower bounds to the reinforcement length for a variety of internal friction angles of the soil, and for different seismic coefficients, k_h.

Figure (9) is a dimensionless design chart for determining the required reinforcement length l/H to prevent the failure of a vertical uniformly reinforced slope for different intensities of seismic coefficient k_h. The Figure also shows the effect of the soil friction angle ϕ on the required normalized length for slopes with angles 80° and 90°. It constitutes a solution to Eq. (10). For a given ϕ, k_h and H, the required l can be estimated using this diagram. It should be noted that the failure mode has been assumed as Figure (2d) in 2D conditions. In other words, the lengths are determined so that the reinforcements do not pull out before they collapse.

It is clearly demonstrated in Figure (9) that both ϕ and k_h have significant effects on the required length of the soil reinforcement. Generally, the required length increases with a decrease in the internal friction angle and an increase in the seismic coefficient k_h. This is consistent with this fact that the lower the value of ϕ and the larger the value of k_h, the more the possibility of failure.

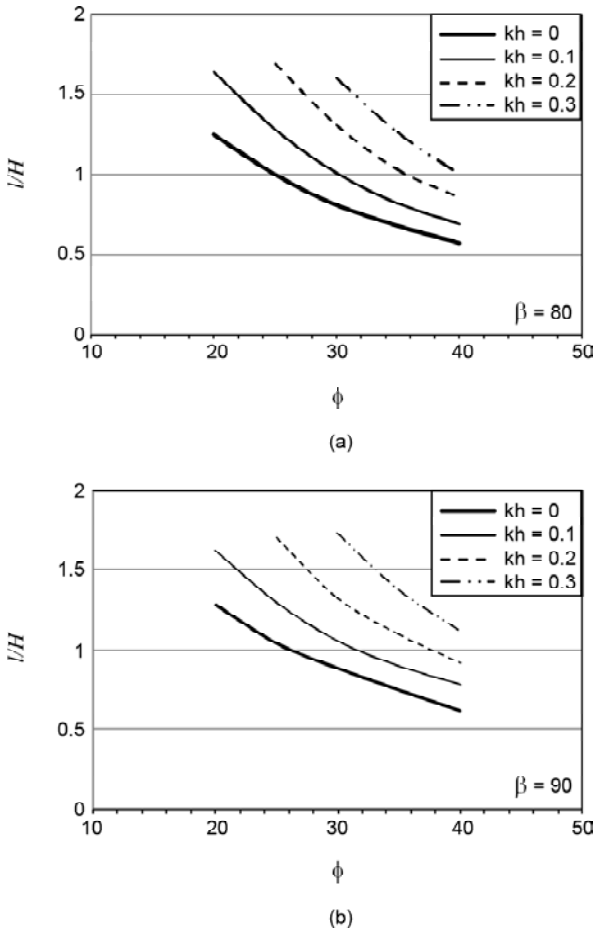

Figure 9. Dimensionless required reinforcement length l/H to prevent the failure of a uniformly reinforced slope for different seismic coefficients kh: (a) β = 80° (b) β = 90°.

To illustrate the effect of the internal friction angle ϕ more quantitavely, it can be seen that for horizontal acceleration coefficient k_h equal to 0.1, when ϕ changes from 20° to 30°, the value of dimensionless required reinforcement length l/H decreases by about 35%. Similarly, when ϕ changes from 30° to 40°, the required value of l/H decreases by about 26%. For k_h = 0.3 when ϕ changes from 30° to 40°, the required value of l/H decreases by about 35%.

7. Required Reinforcement in 3D Cases

Figures (10) and (11) present the variation of the dimensionless parameter k_{3d}/k_{2d} (ratio of k_t in 3D analyses to k_t in 2D analyses) as a function of L/H (L being the width of the failure mechanism) for a reinforced slope with β = 80°. Results are shown for two different values of seismic horizontal coefficients 0 and 0.2. Following results can be obtained from these Figures:

1. The value of k_{3d}/k_{2d} is always lower than unity. In other words, in 3D conditions, the required reinforcements decrease. For example, for L/H= 2, k_h = 0 and ϕ = 20°, the ratio k_{3d}/k_{2d} is 0.88, meaning that the required value of the reinforcement force in 3D condition decreases by about 12%.
2. An increase in the soil internal friction increases the 3D effects. In example discussed above, (L/H= 2, k_h = 0 and ϕ = 20°), when increases from 20° to 30°, the ratio k_{3d}/k_{2d} decreases from 88% to 85%. Of course, this increase is not very considerable.
3. An increase in the horizontal coefficient of acceleration increases the 3D effects. In example discussed in 1 (L/H = 2, k_h = 0 and ϕ = 20°), when k_h increases from 0 to 0.2, the ratio k_{3d}/k_{2d} decreases from 88% to 82%. This effect may be seen much better in Figure (12). In this figure, the parameter 1- k_{3d}/k_{2d} is presented as a function of L/H. k_{3d}/k_{2d} is replaced by 1- k_{3d}/k_{2d} in order for 3D effects to be shown better. This figure is illustrated for a vertical slope with ϕ = 35°. As it is shown, for L/H= 1 when k_h increases from 0 to 0.3, the ratio 1- k_{3d}/k_{2d} increases from 43% to 60%, which is considerable.

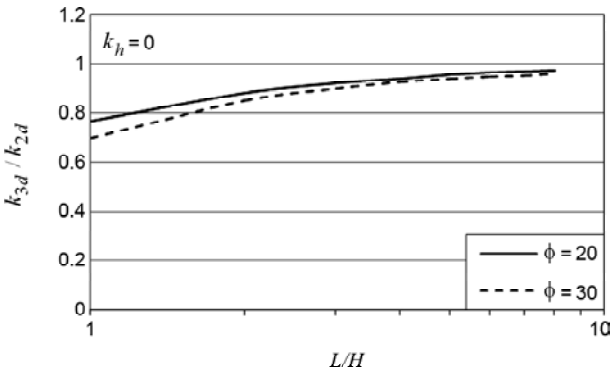

Figure 10. Required reinforcement strength for kh = 0 (β = 80°).

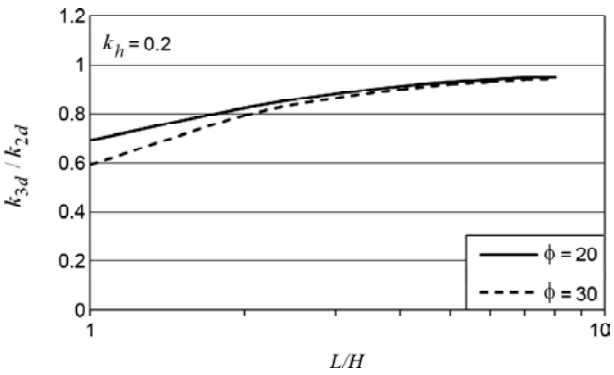

Figure 11. Required reinforcement strength for kh = 0.2 (β = 80°).

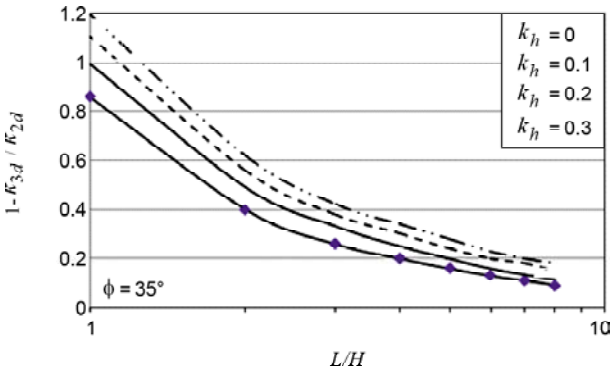

Figure 12. Required reinforcement strength 1- k_{3d}/k_{2d} for different values of kh (β = 90°).

8. Final Remarks

Seismic stability of reinforced soil slopes in three-dimensional conditions has been investigated using a pseudo-static method and upper bound theorem of the limit analysis, incorporating the method of horizontal slices.

First, the theoretical kinematical model of the reinforced soil was described. A comparison of some other analytical results with predictions of the present model was shown and briefly discussed. The conclusion is that the formulation proposed gives realistic predictions.

Effects of soil friction angle, horizontal seismic acceleration, and 3D modeling of the slope was shown and discussed on required reinforcement. It seems that the results shown in figures can be useful in engineering applications because of their simple form, at least to estimate the required reinforcement for real slopes.

The most important results of the present analyses can be summarized as follows:

1. Comparisons of the results presented in this

paper with available pseudo-static methods yielded to satisfactory agreement.
2. The horizontal seismic acceleration is an important parameter for computation of the required length and tensile strength of the reinforcement. Moreover, its importance increases as the earthquake intensity increases.
3. Consideration of the 3D effects result in decreases in the required reinforcement.
4. Three-dimensional effect increases by an increase in soil internal friction. However, this increase may not be considerable.
5. Three-dimensional effect increases much more by the increase in horizontal coefficient of acceleration.
6. As the seismic stability of the reinforced slope reduces with an increase in k_h and greater length, and tensile strength of the reinforcement is required for safe design of reinforced slopes in seismic conditions, use of 3D models in calculation of the required reinforcement may be considered more important by increasing in horizontal coefficient of acceleration.

References

1. Ling, H.I., Leshchinsky, D., and Perry, E.B. (1997). Seismic Design and Performance of Geosynthetic-Reinforced Soil Structures, *Geotechnique*, **47**(5), 933-952.

2. Nouri, H., Fakher, A., and Jones, C.J.F.P. (2006). Development of Horizontal Slice Method for Seismic Stability Analysis of Reinforced Slopes and Walls, *Geotextiles and Geomembranes*, **24**(3), 175-187.

3. Michalowski, R.L. (1997). Stability of Uniformly Reinforced Slopes, *Journal of Geotechnical and Geoenvironmental Engineering*, **123**(6), 546-556.

4. Michalowski, R.L. (1998). Soil Reinforcement for Seismic Design of Geotechnical Structures, *Computers and Geotechnics*, **23**(1), 1-17.

5. Shahgholi, M., Fakher, A., and Jones, C.J.F.P. (2001). Horizontal Slice Method of Analysis, *Geotechnique*, **51**(10), 881-885.

6. Kramer, S.L. and Paulsen, S.B. (2004). Seismic Performance Evaluation of Reinforced Slopes, Geosynthetics International, **11**(6), 429-438.

7. El-Emam, M.M. and Bathurst, R.J. (2005). Facing Contribution to Seismic Response of Reduced-Scale Reinforced Soil Walls, *Geosynthetics International*, **12**(5), 215-238.

8. Huang, C.C. and Wang, W.C. (2005). Seismic Displacement Charts for the Performance-Based Assessment of Reinforced Soil Walls, *Geosynthetics International*, **12**(4), 176-190.

9. Shukla, S., Sivakugan, N., and Das, B. (2011). A State-of-the-Art Review of Geosynthetic-Reinforced Slopes, *International Journal of Geotechnical Engineering*, **5**(1), 17.

10. Li, X., He, S., and Wu, Y. (2012). Limit Analysis of the Stability of Slopes Reinforced with Anchors, *International Journal for Numerical and Analytical Methods in Geomechanics*, **36**(17), 1898-1908.

11. Jiang, Y.P., Chen, Z.Z., Bi, G., and Jiang, X. (2012). Research on Critical Height and Stability of Slopes Based on Upper Bound Limit Analysis Method, *Hydrogeology and Engineering Geology*, **39**(2), 43-46.

12. Ghanbari, A. and Taheri, M. (2012). An Analytical Method for Calculating Active Earth Pressure in Reinforced Retaining Walls Subject to a Line Surcharge, *Geotextiles and Geomembranes*, **34**, 1-10.

13. Vieira, C.S., de Lurdes Lopes, M., and Caldeira, L.M. (2013). Limit Equilibrium Analyses for Internal Design of Geosynthetic Reinforced Slopes: Influence of Potential Failure Surface and Strength Distribution, *Geotechnical and Geological Engineering*, 1-13.

14. Michalowski, R.L. (1989). Three-Dimensional Analysis of Locally Loaded Slopes, *Geotechnique*, **39**(1), 27-38.

15. Chen, Z., Wang, X., Haberfield, C., Yin, J.H., and Wang, Y. (2001). A Three-Dimensional Slope Stability Analysis Method Using the Upper Bound Theorem: Part I: Theory and Methods, *International Journal of Rock Mechanics and Mining Sciences*, **38**(3), 369-378.

16. Farzaneh, O. and Askari, F. (2003). Three-

Dimensional Analysis of Nonhomogeneous Slopes, *Journal of Geotechnical and Geo-environmental Engineering*, **129**(2), 137-145.

17. Li, A.J., Merifield, R.S., and Lyamin, A.V. (2010). Three-Dimensional Stability Charts for Slopes Based on Limit Analysis Methods, *Canadian Geotechnical Journal*, **47**(12), 1316-1334.

18. Lyamin, A.V. and Sloan, S.W. (2002). Lower Bound Limit Analysis Using Nonlinear Programming, *International Journal for Numerical Methods in Engineering*, **55**(5), 573-611.

19. Krabbenhoft, K., Lyamin, A.V., Hjiaj, M., and Sloan, S.W. (2005). A New Discontinuous Upper Bound Limit Analysis Formulation, *International Journal for Numerical Methods in Engineering*, **63**(7), 1069-1088.

20. Zohdi T.H. (2010). Three Dimensional Analysis of Reinforced Soil Slopes with Upper Bound Limit Analysis Method Using Laminar Blocks, M.Sc. thesis, Tehran University, Faculty of Engineering.